

Generic Gravitational Wave Signals from the Collapse of Rotating Stellar Cores

H. Dimmelmeier,^{1,2} C. D. Ott,³ H.-T. Janka,² A. Marek,² and E. Müller²

¹*Department of Physics, Aristotle University of Thessaloniki, GR-54124 Thessaloniki, Greece*

²*Max-Planck-Institut für Astrophysik, Karl-Schwarzschild-Str. 1, D-85741 Garching, Germany*

³*Department of Astronomy and Steward Observatory, University of Arizona, Tucson, AZ 85721, USA*

We perform general relativistic (GR) simulations of stellar core collapse to a proto-neutron star, using a microphysical equation of state (EoS) and an approximation of deleptonization. We show that for a wide range of rotation rates and profiles the gravitational wave (GW) burst signals from the core bounce are generic, known as Type I. In our systematic study, using both GR and Newtonian gravity, we identify and quantify the influence of rotation, the EoS, and deleptonization on this result. Such a generic type of signal templates will facilitate a more efficient search in current and future GW detectors of both interferometric and resonant type.

PACS numbers: 04.25.Dm, 04.30.Db, 95.30.Sf, 95.30.Tg, 95.55.Ym, 97.60.Bw

Theoretical predictions of the gravitational wave (GW) signal produced by the collapse of a rotating stellar iron core to a proto-neutron star (PNS) in a core collapse supernova are complicated, as the emission mechanisms are very diverse. While the prospective GW burst signal from the collapse, bounce, and early postbounce phase is present only when the core rotates [1, 2, 3, 4, 5, 6, 7], one expects GW signals with sizeable amplitudes also from convective motions at later post-bounce phases, anisotropic neutrino emission, excitation of various oscillations in the PNS, or nonaxisymmetric rotational instabilities [7, 8, 9, 10, 11].

In the observational search for GWs from merging binary black holes, powerful data analysis algorithms like matched filtering are applied, as the waveform from the inspiral phase can be modeled very accurately. In stark contrast, the GW burst signal from stellar core collapse and bounce cannot yet be predicted with the desired accuracy and robustness. First, a general relativistic (GR) description of gravity and hydrodynamics including the important microphysics is necessary. Only very few multi-dimensional codes have recently begun to approach these requirements. Second, the rotation rate and profile of the progenitor core are not very strongly constrained. Therefore, the influence of rotation on the collapse dynamics and thus the GW burst signal must be investigated by computationally expensive parameter studies.

Previous simulations, considering a large variety of rotation rates and profiles in the progenitor core but ignoring complex (though essential) microphysics and/or the influence of GR, found qualitatively and quantitatively different types of GW burst signals (see, e.g., [2, 3, 4]). These can be classified depending on the collapse dynamics: *Type I* signals are emitted when the collapse of the homogeneously contracting inner core is not strongly influenced by rotation, but stopped by a *pressure-dominated bounce* due to EoS stiffening at nuclear density ρ_{nuc} where the adiabatic index γ_{eos} rises above 4/3. This leads to instantaneous PNS formation with a maximum core density $\rho_{\text{max}} \geq \rho_{\text{nuc}}$. *Type II* signals occur when centrifugal

forces grow sufficient to halt the collapse, resulting in consecutive (typically multiple) *centrifugal bounces* with intermediate coherent re-expansion of the inner core, seen as density drops by often more than an order of magnitude; thus here $\rho_{\text{max}} < \rho_{\text{nuc}}$ after bounce. *Type III* signals appear in a pressure-dominated bounce when the inner core has a very small mass at bounce due to a soft subnuclear EoS or very efficient electron capture.

In contrast, new GR simulations of rotational core collapse employing a microphysical EoS and an approximation for deleptonization during collapse suggest that the GW burst signature is exclusively of Type I [7]. In this work we considerably extend the number of models and comprehensively explore a wide parameter space of initial rotation states. Also for this more general setup we find GW signals solely of Type I form. We identify the physical conditions that lead to the emergence of this generic GW signal type and quantify their relative influence. Our results strongly suggest that the waveform of the GW *burst* signal from the collapse of rotating supernova cores is much more generic than previously thought.

We perform all simulations in 2+1 GR using the CoCoNuT code [4, 12], approximating GR by the conformal flatness condition (CFC), whose excellent quality in the context of rotational stellar core collapse has been demonstrated extensively (see, e.g., [7, 13]). CoCoNuT utilizes spherical coordinates with the grid setup specified in [7] and assumes axisymmetry. GR hydrodynamics is implemented via finite-volume methods, piecewise parabolic reconstruction, and an approximate Riemann solver. We extract GWs using a variant of the Newtonian quadrupole formula (see, e.g., [13]).

We employ the microphysical EoS of Shen et al. [14, 15]. Deleptonization by electron capture onto nuclei and free protons is realized as in [16]: During collapse the electron fraction Y_e is parameterized as a function of density based on data from spherically symmetric neutrino-hydrodynamic simulations [15] using the latest available electron capture rates [17] (updating recent results [7] where standard capture rates were used). After core

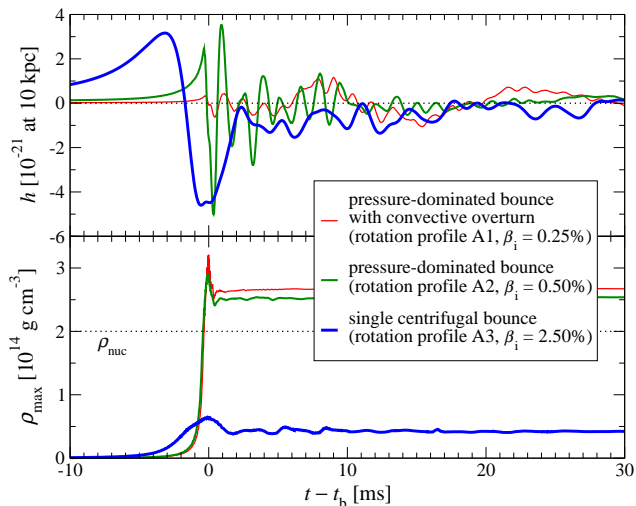


FIG. 1: Time evolution of the GW amplitude h and maximum density ρ_{\max} for three representative models with different rotation profiles and initial rotation rates β_i .

bounce, Y_e is only passively advected and further lepton loss is neglected. Contributions due to neutrino pressure P_ν are taken into account above trapping density [16].

As initial data we take the non-rotating $20 M_\odot$ progenitor s20 from [18], imposing the rotation law discussed in [4, 6]. In order to determine the influence of different angular momentum on the collapse dynamics, we parameterize the initial rotation of our models in terms of the differential rotation parameter A (A1: $A = 50,000$ km, almost uniform; A2: $A = 1,000$ km, moderately differential; A3: $A = 500$ km, strongly differential) and the initial rotation rate $\beta_i = T/|W|$, which is the ratio of rotational energy to gravitational energy (approximately logarithmically spaced in 18 steps from 0.05% to 4%).

As in [7], in the entire investigated parameter space our models yield GW burst signals of Type I, i.e. the waveform exhibits a positive pre-bounce rise and then a large negative peak, followed by a ring-down (upper panel of Fig. 1). However, with respect to collapse dynamics and the relevant forces halting the collapse, the models fall into two classes. While for instance all models with the almost uniform rotation profile A1 experience a pressure-dominated bounce for which a Type I waveform is expected, models with profiles A2 or A3 and sufficiently strong initial rotation rate β_i ($\geq 4\%$ for A2; $\geq 1.8\%$ for A3) show a *single* centrifugal bounce at subnuclear density (lower panel of Fig. 1). Nevertheless, they also produce a Type I waveform, as their core does not re-expand after bounce to densities much less than bounce density but immediately settles to a PNS after a short ring-down phase. What obviously distinguishes models with pressure-dominated bounce from those with centrifugal bounce is that the latter have GW signals with significantly lower average frequencies. Note also that

models with very little rotation develop convective overturn of the shock-heated layer immediately after shock stagnation (not to be confused with the late-time convection discussed in [9]), resulting in a lower-frequency contribution to the post-bounce GW signal (see Fig 1).

In order to analyze the absence of Type II signals, in particular for cases with centrifugal bounce, we now separately investigate the influence of GR, a microphysical EoS, and deleptonization on the dynamics of rotational core collapse with different amounts and distributions of angular momentum. When the pre-collapse iron core starts to contract, its *effective* adiabatic index γ_{eff} is lower than the critical value $\simeq 4/3$ needed for stability against gravitational collapse. Here γ_{eff} is the sum of the adiabatic index $\gamma_{\text{eos}} = \partial \ln P / \partial \ln \rho|_{Y_e, s}$ of the EoS (where P is the pressure, ρ the density, and s the specific entropy of the fluid) and a possible correction due to deleptonization (which can be significant until neutrino trapping; see [2]). At this stage, both GR and rotational effects (in our range of β_i) are negligible in discussing stability. If the build-up of centrifugal forces in the increasingly faster spinning core during collapse is strong enough, contraction is halted and the core undergoes a centrifugal bounce rather than reaching nuclear density (where EoS stiffening would also stop the collapse).

A necessary condition for a centrifugal bounce at subnuclear densities is that γ_{eff} exceeds a critical rotation index γ_{rot} . There exists a simple Newtonian analytic relation, $\gamma_{\text{rot}} = (4 - 10\beta_{\text{ic,b}})/(3 - 6\beta_{\text{ic,b}})$ [19] (where $\beta_{\text{ic,b}}$ is the inner core's rotation rate at bounce), which works well in equilibrium, but is rather imprecise as a criterion for centrifugal bounce in a dynamical situation. For instance, for rotating core collapse models in Newtonian gravity with a simple hybrid EoS [20] and no deleptonization (where $\gamma_{\text{eff}} = \gamma_{\text{eos}}$), we find that for our range of initial rotation rates and $1.24 \leq \gamma_{\text{eff}} \leq 1.332$, the analytic relation strongly underestimates the actual γ_{rot} by up to ~ 0.2 at high $\beta_{\text{ic,b}}$. Furthermore, $\beta_{\text{ic,b}}$ is a result of the evolution, depending on the initial parameters A and β_i of the pre-collapse core in an a-priori unknown way.

For this reason, we determine the boundary between pressure-dominated and centrifugal bounce in terms of the parameters β_i and γ_{eff} by systematic numerical simulations. For models with a simple hybrid EoS [20] and no deleptonization, using the same initial density profile as in the microphysical models, the results are shown in Fig. 2, both in the Newtonian case (dashed lines) and in GR (solid lines). Apparently, for our choice of initial rotation the influence of GR can be approximated by adding an offset of $-\Delta\gamma_{\text{gr}} \simeq 0.015$ to the Newtonian results (dotted lines). This gives a quantitative measure of the GR effects on rotational core collapse, which is in agreement with [4]. Note that $\Delta\gamma_{\text{gr}}$ is negative because GR effectively acts like a softening of the EoS.

Fig. 2 also shows for each rotation profile the locations where the transition between pressure-supported

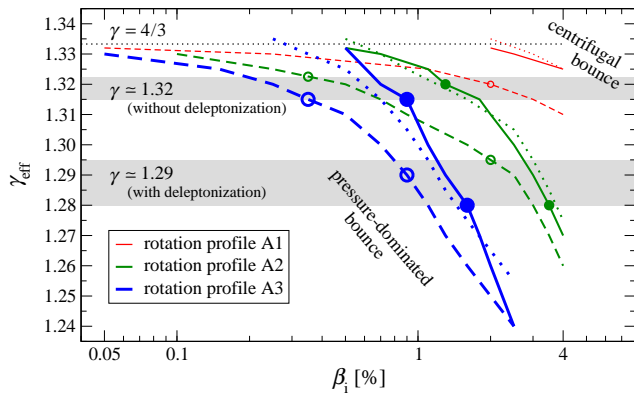


FIG. 2: Boundary between pressure-dominated and centrifugal bounce in the $\gamma_{\text{eff}}-\beta_i$ plane for models using the hybrid EoS in Newtonian gravity (dashed lines) and GR (solid lines). Dotted lines show the Newtonian results shifted by $-\Delta\gamma_{\text{gr}} = 0.015$. The transition points for models using the microphysical EoS without and with deleptonization, again for Newtonian gravity (circles) and GR (bullets), lie in the shaded areas around $\gamma_{\text{eff}} \simeq 1.32$ and 1.29 , respectively.

and centrifugal bounce occurs when the microphysical EoS is used and β_i is gradually increased. These transitions are marked on the different boundary lines and allow the identification of the γ_{eff} value where models with the hybrid EoS make this transition. For simulations with microphysical EoS but no deleptonization we find that in all cases the transition occurs near $\gamma_{\text{eff}} \simeq 1.32$ (highlighted by the upper grey band in Fig. 2). This value agrees with the average of γ_{eos} for the microphysical EoS at densities between 10^{12} and 10^{14} g cm^{-3} , which is the most relevant range for the collapse dynamics. Thus the type of bounce obtained with the microphysical EoS is well reproduced by a hybrid EoS with $\gamma_{\text{eos}} \simeq 1.32$.

Deleptonization before neutrino trapping reduces γ_{eff} compared to γ_{eos} locally according to $\Delta\gamma_e = \frac{4}{3} \delta \ln Y_e / \delta \ln \rho < 0$ [21]. Above trapping an additional positive correction $\Delta\gamma_\nu \approx \delta(P_\nu/P) / \delta \ln \rho$ due to neutrino pressure effects must be considered. From the $Y_e-\rho$ trajectories used to describe the deleptonization during core collapse, we estimate values between -0.03 and -0.02 for $\Delta\gamma_e + \Delta\gamma_\nu$, again in the density regime relevant for the bounce dynamics. Therefore $\gamma_{\text{eff}} \approx 1.29$ is expected for models with microphysical EoS *and* deleptonization. Again this agrees with the simulations. Fig. 2 shows that the circles and bullets marking those models on the different boundary lines (for the investigated initial rotation profiles with Newtonian gravity and GR) all lie in the range of values indicated by the lower grey band.

The finding that deleptonization decreases γ_{eff} to about 1.29 explains the absence of Type II GW signals for our most sophisticated models. When a hybrid EoS is used, the subgroup of such models showing multiple centrifugal bounces and subsequent strong re-expansion phases of the inner core occupies only a small area in the

$\gamma_{\text{eff}}-\beta_i$ plane. It is located at $\gamma_{\text{eff}} \geq 1.31$ for all of our initial rotation states both in the Newtonian case and in GR, i.e. significantly above the value of $\gamma_{\text{eff}} \simeq 1.29$ that characterizes the microphysical models if deleptonization is included.

The value $\gamma_{\text{eff}} = 1.29$ captures well the deleptonization effects in the density regime above neutrino trapping, and therefore models with hybrid EoS and $\gamma_{\text{eos}} = 1.29$ exhibit the same collapse and bounce behavior in this dynamical phase. For $\gamma_{\text{eos}} = 1.29$ the hybrid EoS corresponds to an effective average Y_e of ≈ 0.237 , and thus for models with this EoS we find a small mass $M_{\text{ic}} \sim 0.1-0.3 M_\odot$ of the inner core at bounce (higher for more rapid rotation), consistent with the theory of self-similar collapse [22]. For models with microphysics, however, γ_{eff} is much closer to $4/3$ in the early collapse phase where the initial value of M_{ic} is determined. At intermediate densities below and around neutrino trapping, deleptonization indeed reduces M_{ic} , but only to about $0.5-0.9 M_\odot$, which is in agreement with recent spherically symmetric GR results using Boltzmann neutrino transport [23]. These large values of M_{ic} explain the complete absence of Type III GW burst signals in our models (see also [5]).

The generic nature of the GW burst signal has several important implications for prospective detectability. The limitation to a unique Type I waveform for a very broad range of rotation states of the progenitor core will very likely facilitate the use of more powerful and finetuned data analysis methods in GW detectors. To this end, we offer our results in a waveform catalog [24]. Note that almost all investigated models result in a pressure-dominated bounce and instantaneous formation of a PNS with similar average density and compactness. For these models, whose rotation rates at bounce span two orders of magnitude ($0.2\% \lesssim \beta_{\text{ic,b}} \lesssim 20\%$), the maxima f_{max} of their waveform's frequency spectrum lie in a very narrow range with an average of $\bar{f}_{\text{max}} \simeq 718$ Hz.

This clustering in frequency is reflected in Fig. 3, where we plot the (detector-dependent) frequency-integrated characteristic waveform amplitude h_c against the characteristic frequency f_c (Eq. (31) in [25]) for all 54 GR models with microphysical EoS and deleptonization. We assume optimal orientation of source and detector, and in cases with pressure-dominated bounce remove the lower-frequency contribution from the post-bounce convective overturn by cutting the spectrum below 250 Hz, as we are only interested in the GW signal from the bounce and ring-down. Fig. 3 shows that while current LIGO class interferometric detectors are only sensitive to signals coming from an event in the Milky Way, advanced LIGO could marginally detect some signals from other galaxies in the Local Group like Andromeda. For the proposed EURO detector [26] in xylophone mode, we expect a very high signal-to-noise ratio (which is h_c divided by the detector sensitivity at f_c). This detector could also measure many of the computed signals at a distance of

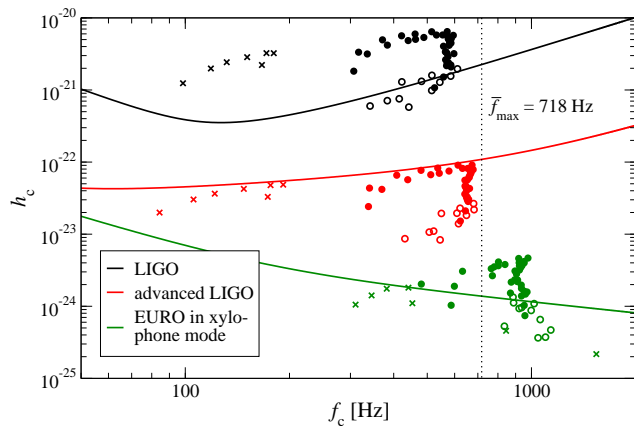


FIG. 3: Location of the GW burst signals from the core bounce for all models in the h_c - f_c plane relative to the sensitivity curves of various GW interferometer detectors (as color-coded). The sources are at a distance of 10 kpc for LIGO, 0.8 Mpc for advanced LIGO, and 15 Mpc for EURO. Open circles denote models where the filtered-out early postbounce convection contributes significantly to the original signal, and crosses show models undergoing centrifugal bounce.

15 Mpc, i.e. in the Virgo cluster.

Note that detectability could be enhanced by (i) a network of interferometers, (ii) the support by resonant detectors, which is facilitated by the narrow range of f_{\max} , and (iii) the use of more powerful data analysis methods based on the waveforms' similarity and robustness. A serious obstacle for detection is the low event rate of $\sim 1 \text{ yr}^{-1}$ within 15 Mpc, which is further reduced by assuming that only a fraction of all progenitors rotate fast enough to have a strong GW bounce signal. Nevertheless, our results can serve as a guideline for a possible frequency narrow-banding of future interferometers (which can significantly boost sensitivity), as well as for choosing the optimal configuration in the planning of resonant detectors. In addition, as a core collapse may be accompanied by other GW emission mechanisms like late-time convection (also in a nonrotating core) or bar-mode instabilities, the *total* GW signal strength and duration could be significantly higher than predicted here.

As a downside, the generic properties of the GW burst signal introduce a frequency degeneracy into the signal inversion problem. Consequently, in the case of a detection it is difficult to extract details about the rotation state of the pre-collapse core, because a large part of the corresponding parameter space yields a pressure-dominated bounce and thus signals with very similar values for f_{\max} and (depending on the detector) also for f_c . On the other hand, as f_{\max} directly depends on the

compressibility of the nuclear EoS at bounce, determining this frequency from the GW burst signal can help to constrain the EoS properties around nuclear density.

We thank D. Shoemaker for helpful discussions. This work was supported by DFG (SFB/TR 7 and SFB 375).

-
- [1] E. Müller, *Astron. Astrophys.* **114**, 53 (1982).
 - [2] R. Mönchmeyer, G. Schäfer, E. Müller, and R. Kates, *Astron. Astrophys.* **246**, 417 (1991).
 - [3] T. Zwerger and E. Müller, *Astron. Astrophys.* **320**, 209 (1997).
 - [4] H. Dimmelmeier, J. Font, and E. Müller, *Astron. Astrophys.* **393**, 523 (2002).
 - [5] K. Kotake, S. Yamada, and K. Sato, *Phys. Rev. D* **68**, 044023 (2003).
 - [6] C. D. Ott, A. Burrows, E. Livne, and R. Walder, *Astrophys. J.* **600**, 834 (2004).
 - [7] C. D. Ott, H. Dimmelmeier, A. Marek, H.-T. Janka, I. Hawke, B. Zink, and E. Schnetter, *Phys. Rev. Lett.* (2006), submitted.
 - [8] M. Rampp, E. Müller, and M. Ruffert, *Astron. Astrophys.* **332**, 969 (1998).
 - [9] E. Müller, M. Rampp, R. Buras, H.-T. Janka, and D. H. Shoemaker, *Astrophys. J.* **603**, 221 (2004).
 - [10] M. Shibata and Y.-I. Sekiguchi, *Phys. Rev. D* **71**, 024014 (2005).
 - [11] C. D. Ott, A. Burrows, L. Dessart, and E. Livne, *Phys. Rev. Lett.* **96**, 201102 (2006).
 - [12] H. Dimmelmeier, J. Novak, J. A. Font, J. M. Ibáñez, and E. Müller, *Phys. Rev. D* **71**, 064023 (2005).
 - [13] M. Shibata and Y.-I. Sekiguchi, *Phys. Rev. D* **69**, 084024 (2004).
 - [14] H. Shen, H. Toki, K. Oyamatsu, and K. Sumiyoshi, *Prog. Theor. Phys.* **100**, 1013 (1998).
 - [15] A. Marek, H.-T. Janka, R. Buras, M. Liebendörfer, and M. Rampp, *Astron. Astrophys.* **443**, 201 (2005).
 - [16] M. Liebendörfer, *Astrophys. J.* **633**, 1042 (2005).
 - [17] K. Langanke and G. Martínez-Pinedo, *Nucl. Phys. A* **673**, 481 (2000).
 - [18] S. E. Woosley, A. Heger, and T. A. Weaver, *Rev. Mod. Phys.* **74**, 1015 (2002).
 - [19] J. E. Tohline, *Astrophys. J.* **285**, 721 (1984).
 - [20] H.-T. Janka, T. Zwerger, and R. Mönchmeyer, *Astron. Astrophys.* **268**, 360 (1993).
 - [21] K. A. van Riper and J. M. Lattimer, *Astrophys. J.* **249**, 270 (1981).
 - [22] A. Yahil, *Astrophys. J.* **265**, 1047 (1983).
 - [23] W. R. Hix, O. E. B. Messer, A. Mezzacappa, M. Liebendörfer, J. Sampaio, K. Langanke, D. J. Dean, and G. Martínez-Pinedo, *Phys. Rev. Lett.* **91**, 201102 (2003).
 - [24] www.mpa-garching.mpg.de/rel_hydro/wave_catalog.shtml
 - [25] K. S. Thorne, in *300 Years of Gravitation*, edited by S. W. Hawking and W. Israel Cambridge University Press, Cambridge, UK, 1987), p. 369.
 - [26] www.astro.cardiff.ac.uk/geo/euro/.